Lattice QCD analysis of the strangeness magnetic moment of the nucleon

Derek B. Leinweber* and Anthony W. Thomas†
Department of Physics and Mathematical Physics and Special Research Centre for the Subatomic Structure of Matter, University of Adelaide, Australia 5005
(Received 30 December 1999; published 8 September 2000)

The outcome of the SAMPLE experiment suggests that the strange-quark contribution to the nucleon magnetic moment, $G_M^s(0)$, may be greater than zero. This result is very difficult to reconcile with expectations based on the successful baryon magnetic-moment phenomenology of the constituent quark model. We show that careful consideration of chiral symmetry reveals some rather unexpected properties of QCD. In particular, it is found that the valence *u*-quark contribution to the magnetic moment of the neutron can differ by more than 50% from its contribution to the Ξ^0 magnetic moment. This hitherto unforeseen result leads to the value $G_M^s(0) = -0.16 \pm 0.18$ with a systematic error, arising from the relatively large strange quark mass used in existing lattice calculations, that would tend to shift $G_M^s(0)$ towards small positive values.

PACS number(s): 12.38.Gc, 12.38.Lg, 13.40.Gp

I. INTRODUCTION

The SAMPLE Collaboration recently reported [1] a new experimental measurement of the strange-quark contribution to the nucleon magnetic moment, $G_M^s(0)$:

$$G_M^s(0.1\ \ \mathrm{GeV}^2) = +0.61 \pm 0.17 \pm 0.21 \mu_N . \qquad (1)$$

We note that the convention for G_M^s is that the negative charge of the strange-quark is not included in the definition. While the uncertainties of the measurement and its interpretation (especially the radiative corrections [2]) are somewhat large and do not totally exclude negative values, this result suggests that $G_M^s(0)$ is quite likely positive. Prior to the appearance of the SAMPLE result most theoretical analyses suggested that $G_M^s(0)$ should be significantly below zero.

An analysis of the result of the SAMPLE experiment within the framework of lattice QCD [3], led to the conclusion that a positive value for $G_M^s(0)$ is extremely difficult to reconcile with our intuitive expectations based on the constituent quark model. In the light of the confirmation of the earlier SAMPLE result, we have been led to reconsider this analysis taking into account the recent progress in incorporating chiral corrections into the extrapolation of quantities such as magnetic moments and masses calculated on the lattice [5–9]. We find that once the correct chiral behavior of lattice quantities is taken into account $G_M^s(0)$ tends to be small and may even be slightly positive. However, in contrast with naive expectations, the effective magnetic moments of the quarks are no longer universal quantities but show a significant dependence on the hadronic environment.

Our investigation begins with the derivation of magnetic moment sum rules for the contributions to octet-baryon magnetic moments from topologically distinct diagrams arising in lattice QCD. These sum rules are *exact* consequences of charge symmetry (i.e., when the light *u* and *d* current quark masses are equal and electromagnetic corrections negligible). As charge symmetry has been shown to be extremely reliable for strongly interacting systems [4], we believe this is a very good approximation. Next we focus on chiral symmetry and the consequent nonanalytic dependence of the baryon magnetic moments on the mass of the light quarks. In particular, we show that the pion cloud contribution enhances the component of the magnetic moment of the neutron associated with the *u*-quark by 50% compared with that associated with the *u*-quark in the Ξ^0; a substantial departure from the common expectation of equal contributions. As we will see, this is precisely the condition required to accommodate $G_M^s(0) > 0$.

The outline of this paper is as follows. Section II briefly reviews the principles behind the derivation of the lattice QCD magnetic moment sum rules [3] and explores the numerical consequences, especially the parameter regions within which G_M^s can be positive. In Sec. III we examine the chiral behavior of the quantities appearing in the sum rules, including their effects on the numerical results. In particular, we show that the effect of the chiral corrections is to move the lattice predictions in precisely the direction required to make $G_M^s(0)$ small in magnitude and possibly positive; our best estimate is $G_M^s(0) = -0.16 \pm 0.18$. In the final section we discuss the results and make some concluding remarks.

II. QCD CONSTRAINTS ON CONTRIBUTIONS TO BARYON MAGNETIC MOMENTS

A. Valence versus sea quarks in baryons

The Euclidean path integral formulation of quantum field theory is the origin of fundamental approaches to the study of quantum chromodynamics (QCD) in the nonperturbative regime. An examination of the symmetries manifest in the QCD path integral for current matrix elements reveals various relationships among the quark sector contributions [3]. As we will see, these relationships, together with the constraints of charge symmetry (which should be very accurate) are sufficient to express the strange-quark contribution to the nucleon magnetic moment, $G_M^s(0)$, in terms of the experi-

*Email address: dleinweb@physics.adelaide.edu.au
†Email address: athomas@physics.adelaide.edu.au

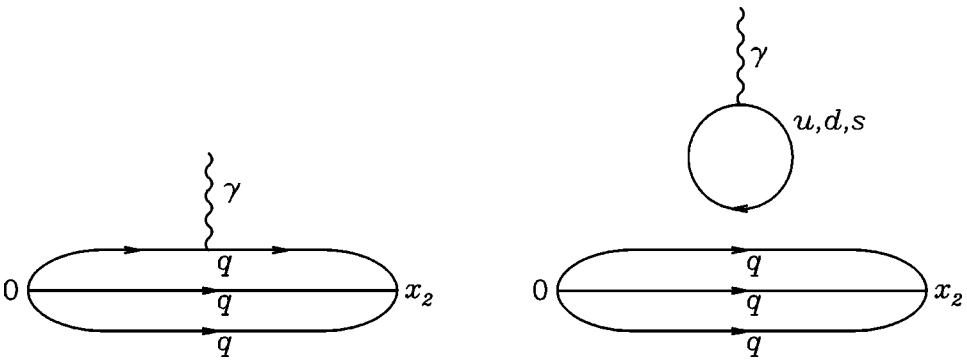

FIG. 1. Diagrams illustrating the two topologically different insertions of the current within the framework of lattice QCD. These skeleton diagrams for the connected (left) and disconnected (right) current insertions may be dressed by an arbitrary number of gluons and quark loops.

mentally measured baryon magnetic moments of p, n, Σ^+, Σ^-, Ξ^0, and Ξ^-, and two ratios of quark contributions to magnetic moments.

We begin by clearly defining the nature of the various quark sector contributions referred to throughout this manuscript. We stress that our theoretical analysis is made within the framework of full (unquenched) QCD, so the line diagrams should be understood as including any number of quark loops and gluons. For our purposes the most important division to define is that between the ''sea''-quark and ''valence''-quark contributions to the magnetic moment of a baryon.

Current matrix elements of hadrons, such as the magnetic moment of the proton, are extracted from the three-point function, a time-ordered product of three operators [3]. Generally, an operator exciting the hadron of interest from the QCD vacuum is followed by the current of interest, which in turn is followed by an operator annihilating the hadron back to the QCD vacuum. In calculating the three point function, one encounters two topologically different ways of performing the electromagnetic current insertion. Figure 1 displays skeleton diagrams for these two possible insertions (with Euclidean time increasing to the right). (As already noted these diagrams may be dressed with an arbitrary number of gluons and quark loops.) The left-hand diagram illustrates the connected insertion of the current to one of the ''valence''[1] quarks of the baryon. In the right-hand diagram the external field produces a $q\bar{q}$ pair which in turn interacts with the valence quarks of the baryon via gluons. It is important to realize that within the lattice QCD calculation of the loop diagram on the right in Fig. 1 there is no antisymmetrization (Pauli blocking) of the quark in the loop with the valence quarks. For this reason, in general *only the sum of the two processes in Fig. 1 is physical*.

The ratios of contributions to the magnetic moment of the nucleon which are directly relevant to the determination of the strangeness magnetic moment include the ratio of the loops (right-hand side of Fig. 1) involving s and d quarks and one of two ratios of valence quark contributions (left hand side of Fig. 1); either the ratio u_p/u_{Σ^+} (expressing the ratio of the valence u-quark contribution in the proton to the analogous contribution when the u-quark resides in the Σ baryon), or the ratio u_n/u_{Ξ^0} (expressing the contribution of a valence u-quark to the neutron relative to that when the u quark resides in the Ξ^0). Within simple constituent quark models, the s/d quark loop ratio is given by a ratio of constituent quark masses [3] to be of order 0.65, while the valence-quark ratios of interest here are equal to unity (i.e., $u_p/u_{\Sigma^+}=u_n/u_{\Xi^0}=1$).

B. QCD equalities

Under the assumption of charge symmetry (namely equal mass light quarks, $m_u=m_d$, and negligible electromagnetic corrections), the three-point correlation functions for octet baryons leads to the following equalities for electromagnetic current matrix elements [3]:

$$p=e_u u_p+e_d d_p+O_N, \qquad n=e_d u_p+e_u d_p+O_N,$$

$$\Sigma^+=e_u u_{\Sigma^+}+e_s s_\Sigma+O_\Sigma, \quad \Sigma^-=e_d u_{\Sigma^+}+e_s s_\Sigma+O_\Sigma,$$

$$\Xi^0=e_s s_\Xi+e_u u_{\Xi^0}+O_\Xi, \quad \Xi^-=e_s s_\Xi+e_d u_{\Xi^0}+O_\Xi. \quad (2)$$

Here, O denotes the contributions from the quark-loop sector—shown on the right-hand side of Fig. 1. The baryon label represents the magnetic moment. Subscripts allow for environment sensitivity implicit in the three-point function [3]. For example, the three-point function for Σ^+ is the same as for the proton, but with d replaced by s. Hence, the u-quark propagators in the Σ^+ are multiplied by an s-quark propagator, whereas in the proton the u-quark propagators are multiplied by a d-quark propagator. The different mass of the neighboring quark gives rise to an environment sensitivity in the u-quark contributions to observables, which means that the naive expectations $u_p/u_{\Sigma^+}=u_n(\equiv d_p)/u_{\Xi^0}=1$ may not be satisfied [3,13–18]. This observation should be contrasted with the common assumption that the quark magnetic moment is an intrinsic-quark property which is independent of the quark's environment.

Focusing now on the nucleon, we note that for magnetic properties, O_N contains sea-quark-loop contributions from primarily u, d, and s quarks. In the SU(3)-flavor limit ($m_u=m_d=m_s$) the charges add to zero and hence the sum van-

[1]Note that the term ''valence'' used here differs from that commonly used in the framework of deep-inelastic scattering. Here ''valence'' simply describes the quark whose quark flow line runs continuously from $0\to x_2$. These lines can flow backwards as well as forwards in time and therefore have a sea contribution associated with them [10].

ishes. However, the heavier strange quark mass allows for a result which is non-zero. By definition

$$O_N = \frac{2}{3}\,{}^lG_M^u - \frac{1}{3}\,{}^lG_M^d - \frac{1}{3}\,{}^lG_M^s, \tag{3}$$

$$= \frac{{}^lG_M^s}{3}\left(\frac{1-{}^lR_d^s}{{}^lR_d^s}\right),$$

$$\text{where } {}^lR_d^s \equiv \frac{{}^lG_M^s}{{}^lG_M^d}, \tag{4}$$

and the leading superscript, l, reminds the reader that the contributions are loop contributions. Note that, in deriving Eq. (4), we have set ${}^lG_M^u = {}^lG_M^d$, corresponding to $m_u = m_d$ [3]. In the constituent quark model ${}^lR_d^s = m_d/m_s \simeq 0.65$. However, we will consider ${}^lR_d^s$ in the range -2 to 2.

With no more than a little accounting, the quark-loop contributions to the nucleon magnetic moment, O_N, may be isolated from Eq. (2) in the following two phenomenologically useful forms:

$$O_N = \frac{1}{3}\left\{2\,p + n - \frac{u_p}{u_{\Sigma^+}}(\Sigma^+ - \Sigma^-)\right\}, \tag{5}$$

$$O_N = \frac{1}{3}\left\{p + 2\,n - \frac{u_n}{u_{\Xi^0}}(\Xi^0 - \Xi^-)\right\}. \tag{6}$$

As we explained above, under the assumption that quark magnetic moments are not environment dependent, these ratios (i.e. u_p/u_{Σ^+} and u_n/u_{Ξ^0}) are taken to be one in many quark models. However, in order to explore the validity of this assumption we will consider the range 0 to 2. Equating (4) with (5) or (6) yields

$$G_M^s = \left(\frac{{}^lR_d^s}{1-{}^lR_d^s}\right)\left[2p + n - \frac{u_p}{u_{\Sigma^+}}(\Sigma^+ - \Sigma^-)\right], \tag{7}$$

and

$$G_M^s = \left(\frac{{}^lR_d^s}{1-{}^lR_d^s}\right)\left[p + 2n - \frac{u_n}{u_{\Xi^0}}(\Xi^0 - \Xi^-)\right]. \tag{8}$$

Incorporating the experimentally measured baryon moments leads to

$$G_M^s = \left(\frac{{}^lR_d^s}{1-{}^lR_d^s}\right)\left[3.673 - \frac{u_p}{u_{\Sigma^+}}(3.618)\right], \tag{9}$$

and

$$G_M^s = \left(\frac{{}^lR_d^s}{1-{}^lR_d^s}\right)\left[-1.033 - \frac{u_n}{u_{\Xi^0}}(-0.599)\right], \tag{10}$$

where all moments are expressed in nuclear magnetons (μ_N). (Note that the measured magnetic moments are all known sufficiently accurately [12] that the experimental errors play no role in our subsequent analysis.) We stress that *these expressions for G_M^s are exact consequences of QCD, under the assumption of charge symmetry*. Equation (10) provides a particularly favorable case for the determination of G_M^s with minimal dependence on the valence-quark ratio.

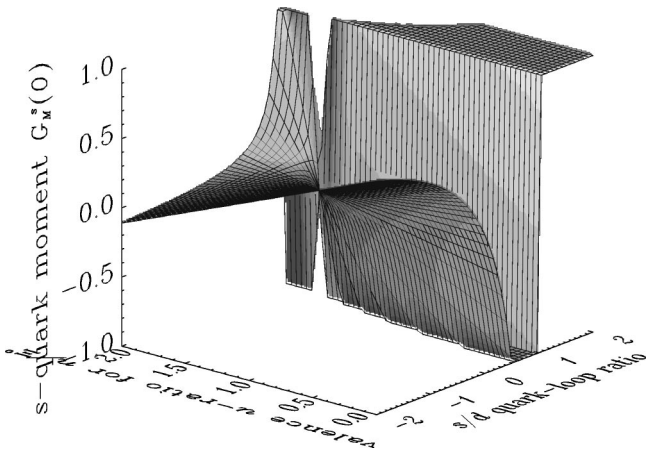

FIG. 2. The surface for $G_M^s(0)$ determined by Eq. (10). Values for $G_M^s(0)$ outside the range $-1 \leqslant G_M^s(0) \leqslant 1$ are constrained to these limits for clarity.

C. Necessary conditions for $G_M^s(0)$ to be positive

Here we investigate the conditions that must hold if $G_M^s(0)$ is to be greater than zero. Since the *s* quark is heavier than the *d* quark, it would be very unusual to find an enhancement in the *s*-quark-loop moment relative to the *d*-quark-loop moment. Such an occurrence would place the loop-ratio ${}^lR_d^s$ greater than one. Likewise, the mass effect is not expected to change the sign of the *s*-quark-loop moment relative to the *d*-quark-loop moment, but rather simply suppress the *s*-quark-loop moment relative to the *d*-quark-loop moment. Hence, the region of interest along the s/d quark-loop ratio axis is the range (0,1) and it would be totally unexpected if the ratio were found to lie outside this range.

Similarly, the success of constituent quark models in explaining the octet-baryon magnetic moments suggests that the ratio of valence *u*-quark moments in the neutron to Ξ^0 should be of order 1. In other words, although the *u* quark is in an environment of two *d* quarks in the neutron and two *s* quarks in Ξ^0, u_n/u_{Ξ^0} is expected to be the order of one. It is important to recall that the main difference between the *n* and Ξ^0 magnetic moments is the difference between the magnetic moment contributions of *s* versus *d* quarks. Traditionally, environment effects are regarded as a secondary effect in the total baryon magnetic moment and often it is completely disregarded. We shall show that, particularly for the minority valence quarks (e.g, the *u* in the neutron), this expectation fails when the effects of chiral symmetry are taken into account.

1. Relation involving u_n/u_{Ξ^0}

We now investigate the range of values of u_n/u_{Ξ^0} and ${}^lR_d^s$ over which Eq. (10) allows positive values of $G_M^s(0)$. Figure 2 illustrates the dependence of $G_M^s(0)$ on these two

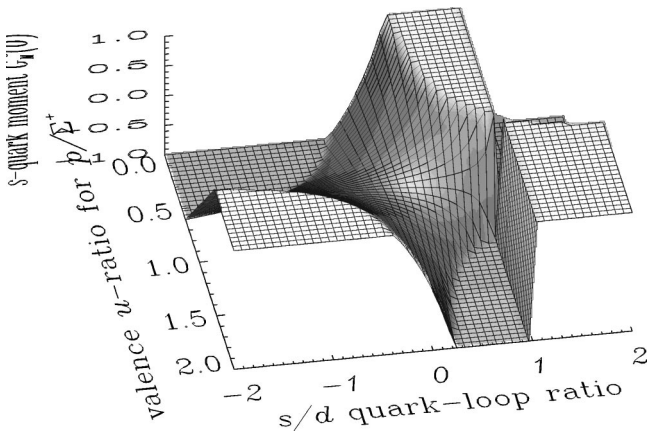

FIG. 3. The surface for $G_M^s(0)$ determined by Eq. (9). Values for $G_M^s(0)$ outside the range $-1 \leqslant G_M^s(0) \leqslant 1$ are constrained to these limits for clarity.

ratios, based on Eq. (10).

Clearly, for the sea-quark-loop ratio, ${}^lR_d^s$, in the expected range (0,1), the valence-quark moment ratio u_n/u_{Ξ^0} must be very large, greater than 1.725. Linear extrapolations of lattice QCD calculations (as a function of quark mass) for this ratio, examining environment sensitivity, lead to a ratio [13,15] $u_n/u_{\Xi^0}=0.72\pm0.46$. This makes the large values required to stay in the region of interest for the sea-quark-loop ratio look somewhat unusual. Because of the nature of the ratios involved, the systematic uncertainties in the actual lattice QCD calculations are expected to be small relative to the statistical uncertainties. Hence the main source of uncertainty is in the extrapolation of the lattice results to the physical world.

2. Relation involving u_p/u_{Σ^+}

Here we study the dependence of $G_M^s(0)$ obtained from Eq. (9) as a function of the quark-sector ratios u_p/u_{Σ^+} and ${}^lR_d^s$. Figure 3 illustrates the value of $G_M^s(0)$, based on Eq. (9), as a function of these two ratios. We see that the solution of Eq. (9) for the sea-quark-loop ratio in the region (0,1) requires the valence-quark moment ratio $u_p/u_{\Sigma^+}<1.015$.

3. Consistency relation

Equating (9) and (10) provides a linear relationship between u_p/u_{Σ^+} and u_n/u_{Ξ^0} which must be satisfied within QCD. Figure 4 displays this relationship by the dashed and solid line, the latter corresponding to values for which $G_M^s(0)>0$ when ${}^lR_d^s$ is in the anticipated range $0<{}^lR_d^s<1$. Since the line does not pass through the point (1.0,1.0) corresponding to the simple quark model assumption, the experimentally measured moments are signaling that there must be an environment effect exceeding 12% in both ratios or approaching 20% or more in at least one of the ratios. Moreover, a positive value for $G_M^s(0)$ requires an environment sensitivity exceeding 70% in the u_n/u_{Ξ^0} ratio.

III. CHIRAL CORRECTIONS

One of the major challenges at present in connecting lattice calculations of hadronic properties with the physical

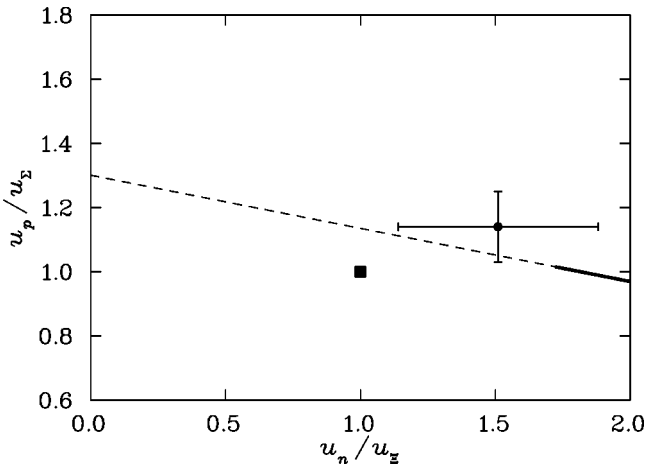

FIG. 4. The consistency relation between u_p/u_{Σ^+} and u_n/u_{Ξ^0} which must be satisfied within QCD. The part of the straight line which is dashed corresponds to $G_M^s(0)<0$, while the solid part of the line has $G_M^s(0)>0$. The standard quark model assumption of intrinsic quark moments independent of their environment is indicated by the filled square. The lattice QCD prediction (after an appropriate chiral extrapolation, discussed in following sections) is illustrated by the filled circle.

world is that computational limitations restrict the accessible quark masses to values an order of magnitude larger than the physical values. At such large masses one is far from the region where chiral perturbation theory is applicable. Yet one knows that for current quark masses near zero there is important non-analytic structure (as a function of the quark mass) which must be treated correctly if we are to compare with physical hadron properties. Our present analysis of the strangeness magnetic form factor has been made possible by a recent breakthrough in the treatment of these chiral corrections for the nucleon magnetic moments [5,6]. In particular, a study of the dependence of the nucleon magnetic moments on the input current quark mass, within a chiral quark model which was fitted to existing lattice data, suggested a model independent method for extrapolating baryon magnetic moments which satisfied the chiral constraints imposed by QCD. We briefly summarize the main results of that analysis.

A series expansion of $\mu_{p(n)}$ in powers of m_π is not a valid approximation for m_π larger than the physical mass. On the other hand, the behavior of the model, after adjustments to fit the lattice data at large m_π is well determined by the simple Padé approximant:

$$\mu_{p(n)}=\frac{\mu_0}{1-\dfrac{\chi}{\mu_0}m_\pi+c\,m_\pi^2}. \tag{11}$$

Equation (11) not only builds in the usual magnetic moment of a Dirac particle at moderately large m_π^2 but has the correct leading non-analytic (LNA) behavior of chiral perturbation theory

$$\mu=\mu_0+\chi\,m_\pi,$$

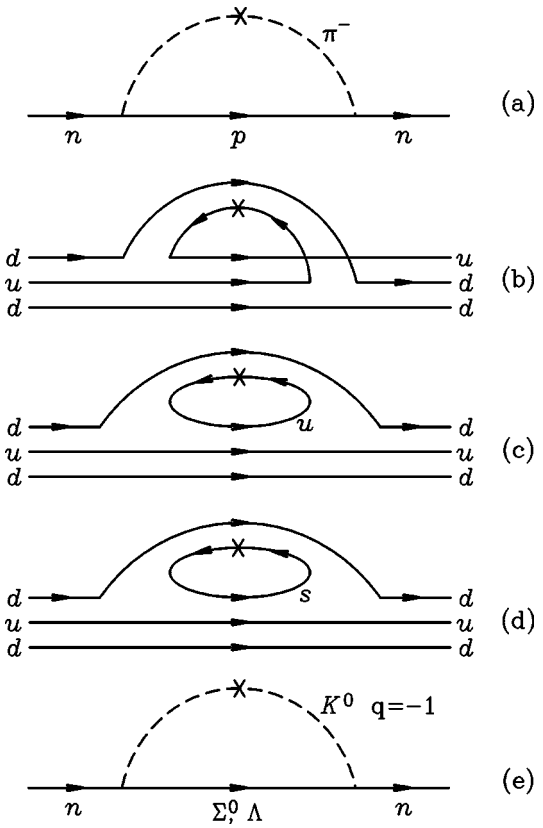

FIG. 5. The components of the leading non-analytic contribution to the magnetic moment of the neutron—(a) through (c), as well as related processes, (d) and (e), with the same chiral behavior as (c).

with χ a model independent constant.

Fixing χ at the value given by chiral perturbation theory and adjusting μ_0 and c to fit the lattice data yielded values of μ_p and μ_n of $2.85 \pm 0.22 \mu_N$ and $-1.96 \pm 0.16 \mu_N$, respectively, at the physical pion mass. These are in remarkably good agreement with the experimental values—certainly much closer than the usual linear extrapolations in m_q.

Clearly it is vital to extend the lattice calculations of the baryon magnetic moments to lower values of m_π than the 600 MeV used in the study just outlined. It is also vital to include dynamical quarks. Nevertheless, the apparent success of the extrapolation procedure gives us strong encouragement to investigate the same approach for resolving the strange quark contribution to the proton magnetic moment.

A. Chiral behavior of the valence and sea contributions

The study of the chiral behavior of hadronic properties calculated on the lattice is still at a relatively early stage of development. For quenched QCD there has been a very thorough investigation of the corrections to hadron masses [11,19]. However, for magnetic moments little is known apart from the constraints of chiral perturbation theory for full QCD. Figure 5(a) illustrates the process which gives rise to the leading non-analytic behavior of the neutron magnetic moment. (The cross represents the electromagnetic current operator.) The breakdown of this process into lattice valence and sea contributions is shown in Figs. 5(b) and (c), respectively. Note that although Fig. 5(b) involves propagation of one of the valence quarks backward in time, its topology is equivalent to that of Fig. 1(a) and it is included in it.

It is important to realize that the separation of Fig. 5(a) into the components (b) and (c), while perfectly reasonable within a lattice formulation of the problem, is not physical. That is, because there is no antisymmetrization exchange between the quark in the loop and the valence quarks in Fig. 5(c), the quantum numbers of the baryons appearing in the intermediate states of Figs. 5(b) and (c) are not necessarily allowed. Only the sum of the two diagrams, in which the unphysical contributions cancel, has a physical meaning. On the other hand, if one is to analyze the baryon magnetic moments within the framework of lattice QCD, as outlined in Sec. II, one must understand the chiral behavior of Figs. 5(b) and (c) separately.

Fortunately this is not so difficult. We know the leading non-analytic (LNA) behavior of the full diagram, Fig. 5(a), so that, if we can calculate the corresponding behavior of either (b) or (c) we know the other. Figure 5(c) involves a u-quark loop where (within the calculational rules for lattice QCD) no exchange term is possible. Thus the u-quark in the loop is distinguishable from all the other quarks in the diagram. The chiral structure of this diagram is therefore identical to that for a ''strange'' quark loop, as illustrated in Fig. 5(d), provided the ''strange'' quark appearing here is understood to have the same mass as the u-quark.

The corresponding hadron diagrams which give rise to the leading non-analytic structure of Fig. 5(c) are therefore those shown in Fig. 5(e), with the distinguishable (''strange'') quark mass set equal to the mass of the u-quark. That is, the intermediate, spin-$\frac{1}{2}$ baryons appearing in Fig. 5(e) should be degenerate with the nucleon. Similarly, the ''kaon'' mass is degenerate with the pion. In addition, it should be reasonable to estimate the coupling constants using SU(6) symmetry—note that in this case all the quarks *do* have the same mass.

As a check of this technique for extracting the LNA behavior, we confirmed that our results for the chiral contribution of the valence term to the mass of the nucleon obtained with our technique agrees with that obtained for quenched QCD, in the more formal approach of Labrenz and Sharpe [11]—after allowing for the η and η' contributions which are unique to the quenched case. (Note that these authors also use SU(6) coupling constants.)

The only residual technique needed is that, in order to pick out the u-quark contribution to these various diagrams—e.g., the quantity ${}^lG_M^u$ appearing in Eq. (4) or u_n in Eq. (10)—we set the electromagnetic charge of the u-quark to be $+1$ in Fig. 5(b) and Fig. 5(c) and the d-quark charge to zero. As the ''strange'' quark of Fig. 5(d) is accounting for the u-quark contribution in Fig. 5(c), this ''strange'' quark also takes charge $+1$. This is the reason for the label $q=-1$ on the ''K^0'' in Fig. 5(e), which ensures that the anti-u-quark in Fig. 5(c) is counted correctly.

The separation of valence and sea u-quark contributions must also be carried out for the process illustrated in Fig. 6. While the net effect of the π^0 cloud is vanishing, valence and loop contributions are equal and opposite in sign. As in

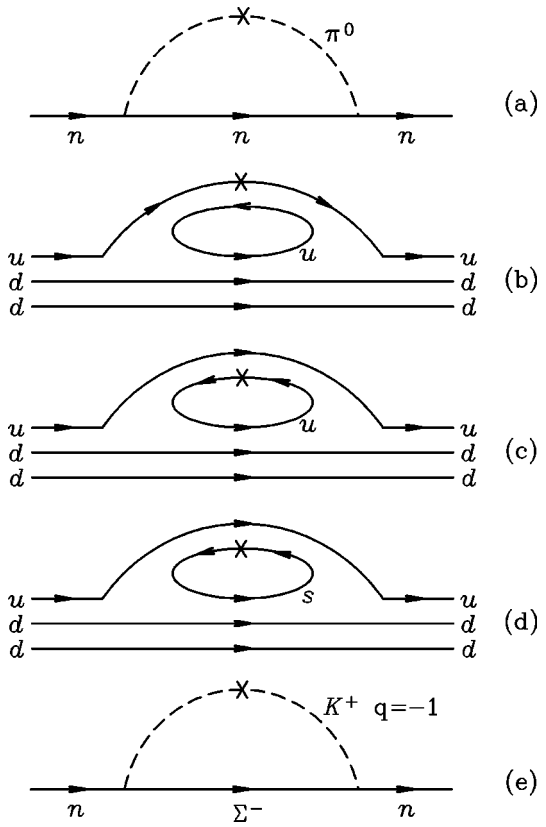

FIG. 6. Separation of valence and sea contributions to the π^0 loop contribution to the magnetic moment of the neutron—(a) through (c). While the net effect is vanishing, valence and sea contributions are equal and opposite in sign. The related processes, (d) and (e), with the same chiral behavior as (c) are discussed in the text.

Fig. 5, Fig. 6(c) involves a *u*-quark loop where no exchange term is possible. Thus the *u*-quark in the loop is essentially distinguishable from all the other quarks in the diagram. The chiral structure of this diagram is identical to that for a strange quark loop, as illustrated in Fig. 6(d), provided the ''strange'' quark appearing here is understood to have the same mass as the *u*-quark. The corresponding hadron diagrams which give rise to the leading non-analytic structure of Fig. 6(c) are therefore those shown in Fig. 6(e), with the distinguishable (''strange'') quark mass set equal to the mass of the *u*-quark. Again, we set the electromagnetic charge of the *u*-quark to be $+1$ and the *d*-quark charge to zero in Fig. 6(b) and (c). As the ''strange'' quark of Fig. 6(d) is accounting for the *u*-quark contribution in Fig. 6(c), this ''strange'' quark also takes charge $+1$ and the *u* and *d* charges are set to zero. In this way the ''K^+'' has charge $q=-1$ in Fig. 6(e), which ensures that the anti-*u*-quark in Fig. 6(c) is counted correctly.

A summary of the isospin and charge factors associated with the leading non-analytic (LNA) chiral coefficients is given in Table I. The LNA pieces of these various contributions to the baryon magnetic moments are proportional to

$$\beta \frac{m_N}{8\pi f_\pi^2} m_\pi \equiv \chi m_\pi, \tag{12}$$

TABLE I. Isospin and charge factors for the leading nonanalytic contribution of the *u*-quark(s) to the magnetic moment of various baryons. The *u*-quark charge has been normalized to 1, as explained in the text. The contribution of the valence quark sector alone is obtained by subtracting the sea-quark loop contribution (''*u*-sea-quark loop'') from the total *u*-flavor sector (''*u*-flavor-sector'').

Baryon	*u*-flavor sector	*u*-sea-quark loop
n	$-2\,f_{\pi NN}^2$	$-(3\,f_{KN\Sigma}^2+f_{KN\Lambda}^2)$
Ξ^0	$+2\,f_{\pi\Xi\Xi}^2$	$-2\,f_{\pi\Xi\Xi}^2$
p	$+2\,f_{\pi NN}^2$	$-(3\,f_{KN\Sigma}^2+f_{KN\Lambda}^2)$
Σ^+	$f_{\pi\Sigma\Sigma}^2+f_{\pi\Sigma\Lambda}^2$	$-(f_{\pi\Sigma\Sigma}^2+f_{\pi\Sigma\Lambda}^2)$

where the pion decay constant $f_\pi=93$ MeV. The coefficients β and χ for various quark sectors and baryons are summarized in Table II. [Note that β and χ are, of course, equivalent but for completeness we give numerical values for both, as well as the analytic expression for β in terms of the SU(6) constants F and D.] The heading ''*u*-flavor-sector'' is the *u*-quark contribution to the LNA behavior of the baryon magnetic moments in full QCD; ''*u*-sea-quark loop'' gives the terms we just discussed [such as Fig. 5(c) and Fig. 6(c)] and ''*u*-valence sector'' is the difference [corresponding, for example, to Fig. 5(b) plus Fig. 6(b)].

For the calculation of $G_M^s(0)$, the LNA chiral behavior of u_n and u_{Ξ^0} is crucial, as the corresponding coefficients are of opposite sign. As a result, the ratio of these *u*-quark contributions, extrapolated with the correct chiral behavior, will be completely different from the linearly extrapolated ratio. That the signs of these chiral coefficients are opposite may be traced back to the charge of the predominant pion cloud associated with these baryons. The chiral behavior in the neutron case is dominated by the transition $n\to p\,\pi^-\to n$, where there is a contribution from a $\bar{u}$ loop. On the other hand, for the Ξ^0 the LNA *u*-quark contribution is dominated by the process $\Xi^0\to\Xi^-\pi^+\to\Xi^0$, shown in Fig. 7. In this case there is no contribution from a *u*-sea-quark loop, rather the virtual π^+ involves a valence *u*-quark—and hence the sign change. Of course, one must account for a *u*-quark loop contribution in the process of Fig. 8, which is completely analogous to Fig. 6.

In Fig. 8(c) we have a *u*-quark loop where, according to the rules of lattice field theory, no exchange term is possible. Thus the *u*-quark in the loop is essentially distinguishable from all the other quarks in the diagram. The chiral structure of this diagram is therefore identical to that for a *d*-quark loop, as illustrated in Fig. 8(d) provided the ''*d*-quark'' appearing here has the same mass as the *u*-quark. It is convenient to use the *d*-quark in this case as it does not appear as one of the valence quark flavors, just as the strange quark could be used earlier because it is not a valence flavor of the neutron.

As a result of these arguments, the hadronic diagrams which give rise to the leading non-analytic structure of Fig. 8(c) are therefore those shown in Fig. 8(e). The electromagnetic charge of the *d*-quark in the loop of Fig. 8(d), accounting for the *u*-quark contribution of Fig. 8(c), is set to $+1$ and

TABLE II. Coefficients β and χ of Eq. (12) for the leading nonanalytic (LNA) contribution of the u-quark(s) to the magnetic moment of various baryons. We express the LNA coefficients χ in terms of the usual SU(6) constants F and D, as well as giving numerical values for χ and β [which are equivalent through Eq. (12)]. The u-quark charge has been normalized to 1, for reasons explained in the text.

Baryon	Coefficient	u-flavor sector	u-sea-quark loop	u-valence sector
n	β	$(F+D)^2$	$(9F^2-6FD+5D^2)/3$	$2(-3F^2+6FD-D^2)/3$
	β	1.020	0.612	0.408
	χ	4.41	2.65	1.76
Ξ^0	β	$-(F-D)^2$	$+(F-D)^2$	$-2(F-D)^2$
	β	-0.0441	0.0441	-0.0882
	χ	-0.191	0.191	-0.381
p	β	$-(F+D)^2$	$(9F^2-6FD+5D^2)/3$	$-4(3F^2+2D^2)/3$
	β	-1.020	0.612	-1.632
	χ	-4.41	2.65	-7.06
Σ^+	β	$-2(3F^2+D^2)/3$	$2(3F^2+D^2)/3$	$-4(3F^2+D^2)/3$
	β	-0.568	0.568	-1.136
	χ	-2.46	2.46	-4.91

all the other quark charges are zero. In this way the ''π^+'' has charge $q=-1$ in Fig. 8(e), which ensures that the anti-u-quark in Fig. 8(c) is counted correctly.

B. Numerical results including chiral behavior

The original lattice QCD studies of the magnetic moments of the octet baryons [13–15] contain enough information that one can readily extract the contributions associated with each flavor of valence quark.

The lattice QCD simulations were performed on a $24\times12\times12\times24$ periodic lattice using standard Wilson actions at $\beta=5.9$. Dirichlet boundary conditions were used for fermions in the time direction. Twenty-eight quenched gauge configurations were generated by the Cabibbo-Marinari [20] pseudo-heat-bath method. The conserved vector current was derived from the Wilson fermion action via the Noether procedure. The associated lattice Ward identity protects this vector current from renormalization. Statistical uncertainties in the lattice simulation results are calculated in a third-order, single elimination jackknife [21,22]. Further details may be found in Ref. [13].

We stress that our theoretical analysis has been based on full QCD, whereas the existing lattice calculations have all been made within quenched QCD. On the other hand, the range of quark masses over which these calculations have been carried out corresponds to pion masses greater than 600 MeV. The study of Refs. [5,6] suggests that at such large masses the errors arising from quenching should be less than 10%, since the *total* pion contribution is of this order. Thus,

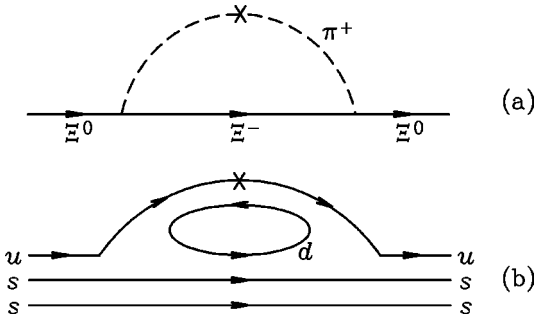

FIG. 7. The dominant leading non-analytic contribution to the magnetic moment of the Ξ^0—see the text for the explanation of process (b).

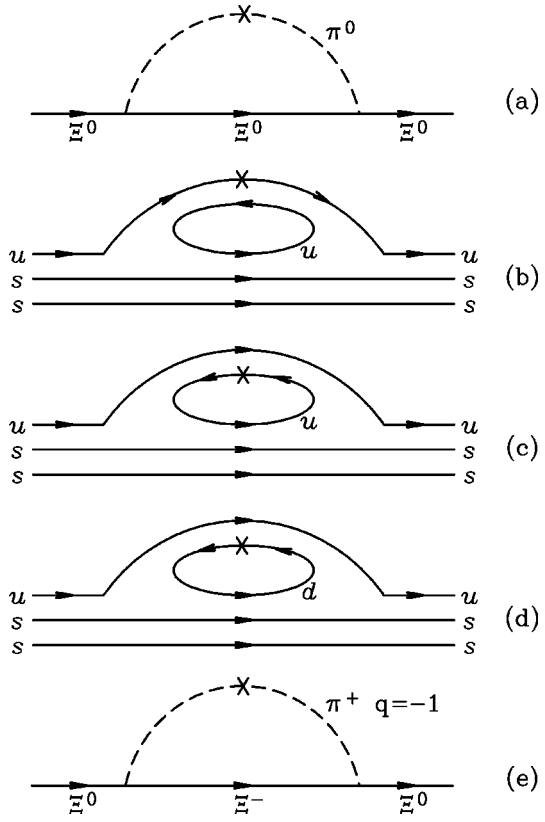

FIG. 8. Separation of valence and sea contributions to the π^0 loop contribution to the magnetic moment of Ξ^0—(a) through (c). The related processes, (d) and (e), with the same chiral behavior as (c) are discussed in the text.

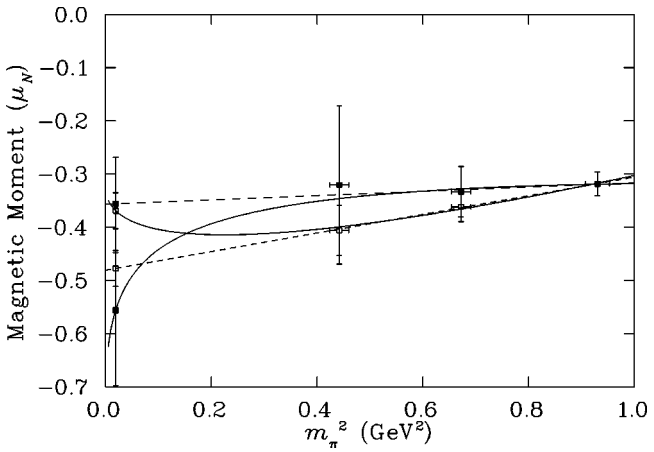

FIG. 9. Extrapolation of the valence *u*-quark magnetic moment contributions to the neutron (solid symbols) and Ξ^0 (open symbols). Naive linear extrapolations (dashed lines) are contrasted with the chiral extrapolations based on Eq. (13) for the neutron and Eq. (14) for Ξ^0. The lattice data is taken from Ref. [13].

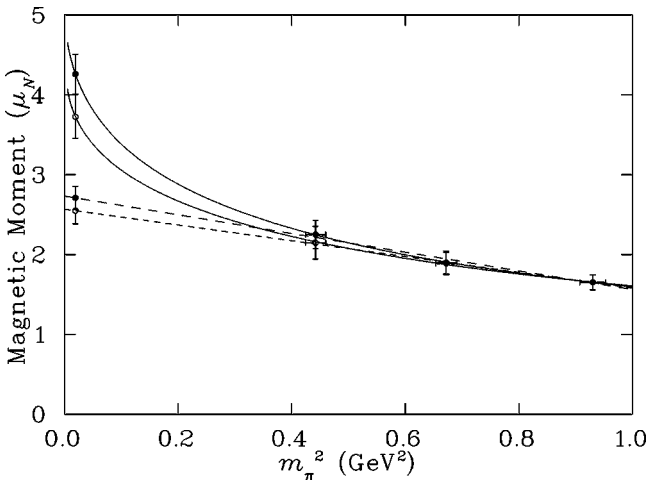

FIG. 10. Extrapolation of the valence *u*-quark magnetic moment contributions to the proton (solid symbols) and Σ^+ (open symbols). Naive linear extrapolations (dashed lines) are contrasted with the chiral extrapolations based on Eq. (13). The lattice data is taken from Ref. [13].

while it would be highly desirable to have full QCD data, we do not expect the errors arising from using the existing quenched data to be unreasonable.

In order to extrapolate the lattice data for valence quarks to the physical pion mass we use the same approach which worked so well for the neutron and proton moments in Refs. [5,6]. That is, we fit the lattice data for the valence quark of flavor q in baryon B with the form

$$\mu(m_\pi) = \frac{\mu^0}{1 - \dfrac{\chi}{\mu^0} m_\pi + c m_\pi^2}. \tag{13}$$

Here χ are the modified LNA chiral coefficients for the valence quarks given in Table II (last column) and μ^0 and c are fitting parameters. In the case of the *u*-quark in Ξ^0, the sign of χ is such that a singularity is introduced in Eq. (13); a feature not present in the standard chiral expansion

$$\mu(m_\pi) \simeq \mu^0 + \chi m_\pi + c m_\pi^2. \tag{14}$$

Fortunately the coefficient χ is small and Eq. (14) should be adequate. Because χ is small, we are able to test the sensitivity of the truncation of the chiral expansion of Eq. (14) by also considering the form

$$\mu(m_\pi) = \frac{\mu^0 + \chi m_\pi}{1 + c m_\pi^3}, \tag{15}$$

which has the correct chiral and heavy quark limits. Extrapolations based on this form agree with Eq. (14) at the 7% level. We present extrapolations based on Eq. (14) in the following.

Figures 9 and 10 illustrate the extrapolations of the lattice data. The results of these fits shown at $m_\pi = 140$ MeV are the results of the extrapolation procedure, including fitting errors. Naive linear extrapolations are also shown to help emphasize the dominant role of chiral symmetry in the extrapolation process.

Clearly the effect of the chiral corrections on the extrapolated values of the key magnetic moment ratio

$$\frac{\mu_u^n(m_\pi = 140\ \text{MeV})}{\mu_u^{\Xi^0}(m_\pi = 140\ \text{MeV})} \tag{16}$$

is dramatic. Instead of the value 0.72 ± 0.46 obtained by linear extrapolation one now finds 1.51 ± 0.37. By comparison, the ratio

$$\frac{\mu_u^p(m_\pi = 140\ \text{MeV})}{\mu_u^{\Sigma^+}(m_\pi = 140\ \text{MeV})} \tag{17}$$

is quite stable, changing from 1.14 ± 0.08 in the case of linear extrapolation to 1.14 ± 0.11 when the correct chiral extrapolation is used. In lattice terminology the u_n/u_{Ξ^0} case involves a ''singly represented'' quark, whereas u_p/u_{Σ^+} involves the ''doubly represented'' quark. It is perhaps not too surprising that the breakdown of the universality of the effective quark magnetic moments should be bigger for the quarks which are in the minority. It is vital that the ratio obtained in Eq. (16) is much more consistent with the range of values found necessary (in Sec. II) to yield a positive value of G_M^s, as illustrated in Fig. 4—values which seemed quite unreasonable in the constituent quark model.

Figures 11 and 12 illustrate the allowed range of G_M^s, using Eqs. (9) and (10) respectively, with these new valence ratios (as a function of the loop ratio ${}^lR_d^s$). Recent calculations [23] place ${}^lR_d^s = 0.55$, and Eqs. (9) and (10) yield $G_M^s = -0.57 \pm 0.42 \mu_N$ and $-0.16 \pm 0.18 \mu_N$, respectively.

As we have already remarked, the effect of the chiral extrapolation on the ratio u_n/u_{Ξ^0} is the most dramatic, changing it from 0.72 ± 0.46 to 1.51 ± 0.37. Thus Eq. (10),

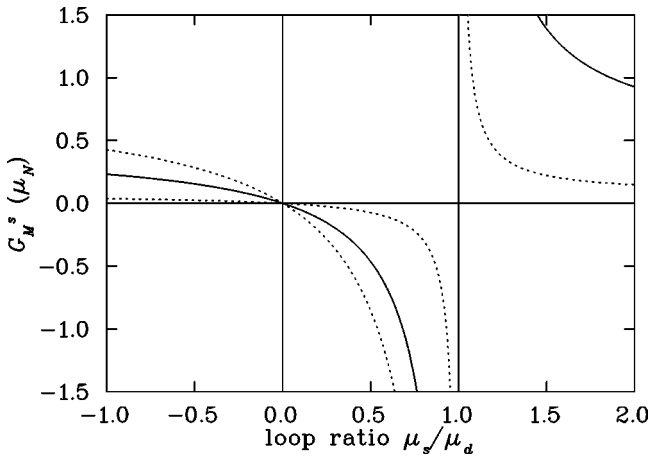

FIG. 11. The strange quark contribution to the nucleon magnetic moment $G_M^s(0)$ obtained from Eq. (9) plotted as a function of ${}^lR_d^s$ reflecting the relative contribution of strange to light sea-quark loop contributions. The solid curve illustrates the central values and the dashed curves denote the standard error.

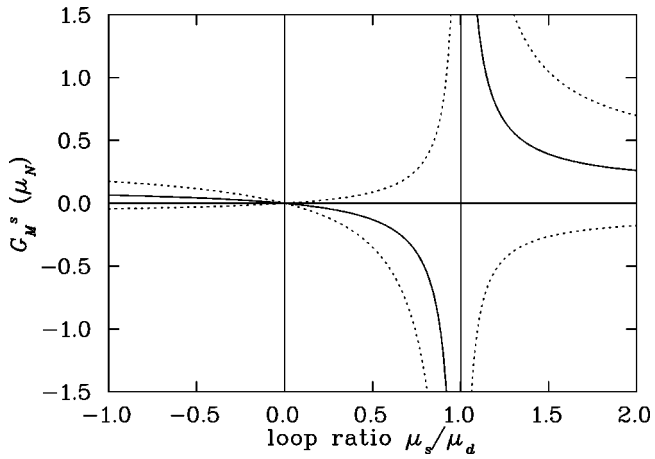

FIG. 12. The strange quark contribution to the nucleon magnetic moment $G_M^s(0)$ obtained from Eq. (10) plotted as a function of ${}^lR_d^s$ reflecting the relative contribution of strange to light sea-quark loop contributions. The solid curve illustrates the central values and the dashed curves denote the standard error.

which seemed certain to guarantee $G_M^s<0$, no longer does. Indeed, we obtain $G_M^s=-0.16\pm0.18\mu_N$. While this is still negative it does permit a small positive value within the error.

IV. SUMMARY REMARKS AND OUTLOOK

We have presented two equations, Eqs. (9) and (10), describing the strange quark contribution to the nucleon magnetic moment, $G_M^s(0)$, in terms of the ratio of strange to light sea-quark-loop contributions and valence-quark ratios which probe the effects of environment sensitivity. These equations are *exact* consequences of QCD under the assumption of charge symmetry (i.e., $m_u=m_d$ and negligible electromagnetic corrections).

The sea-quark-loop ratio probes the quark-mass suppression of the strange-quark loop relative to the light-quark loop such that the ratio is expected to lie between 0 and 1. Traditionally this ratio is given by a ratio of constituent quark masses yielding 0.65 while more recent estimates [23] place it at 0.55.

The valence-quark ratios probe the effects of environment sensitivity. In this discussion we have seen how differences in the pion cloud contributions to various baryons give rise to very significant environment sensitivity in the quark sector contributions to baryon magnetic moments. Indeed the environment sensitivity in the *u*-quark contributions to *n* versus Ξ^0 are so large, $(u_n/u_{\Xi^0}=1.51\pm0.37)$, that one should seriously reconsider the validity of a constituent quark picture for the minority, or ''singly represented'' valence quarks. Using the new value for u_n/u_{Ξ^0} leads to a strangeness magnetic moment for the proton, $G_M^s(0)$, equal to $-0.16\pm0.18\mu_N$.

The lattice QCD simulation results themselves display an environment sensitivity. For example, the strange quarks in the Ξ^0 act to enhance the magnitude of the *u*-quark contribution to the Ξ^0 moment relative to that in the neutron in the simulation results. However, this environment sensitivity may be an overestimate, as the mass of the strange quark used in the lattice QCD simulations is somewhat heavy, approaching 300 MeV.

As an estimate of the effects of this systematic error, we may average the neutron and Ξ^0 simulation results for the *u*-quark to linearly interpolate to a strange quark mass the order of 150 MeV. In this case the magnetic moment ratio, u_n/u_{Ξ^0}, increases to 1.9(6) providing a positive value for $G_M^s(0)$ at $0.09(22)\mu_N$, a shift of $0.25\mu_N$ in the central value. Similarly the u_p/u_{Σ^+} ratio becomes 1.09(10) and provides $G_M^s(0)=-0.35(39)\mu_N$, also consistent with small positive values for $G_M^s(0)$, within one standard deviation. In the absence of new lattice calculations with a realistic strange quark mass, it is not possible to make a better estimate of the systematic error on $G_M^s(0)$. We find it remarkable that the approach described here can produce a reasonably precise estimate of $G_M^s(0)$ from the Ξ^0 and *n* systems even with lattice data that is quite old. Advances in high performance computing and lattice QCD methodology in the last seven to eight years mean that it should be possible to dramatically reduce both the statistical and systematic errors. In view of the present results, and the importance of understanding the role of strangeness in the nucleon, this is clearly an urgent priority—as is the need to obtain unquenched magnetic moment results at masses as low as possible.

ACKNOWLEDGMENTS

We would like to acknowledge very helpful discussions concerning the work described here and particularly this manuscript with Pierre Guichon and Tony Williams. This work was supported by the Australian Research Council.

[1] SAMPLE Collaboration, D. Spayde *et al.*, Phys. Rev. Lett. **84**, 1106 (2000); B. Mueller *et al.*, *ibid.* **78**, 3824 (1997).
[2] M. J. Musolf and B. R. Holstein, Phys. Lett. B **242**, 461 (1990).
[3] D. B. Leinweber, Phys. Rev. D **53**, 5115 (1996).
[4] G. A. Miller, B. M. Nefkens, and I. Slaus, Phys. Rep. **194**, 1 (1990).
[5] D. B. Leinweber, D. H. Lu, and A. W. Thomas, Phys. Rev. D **60**, 034014 (1999).
[6] A. W. Thomas, D. B. Leinweber, and D. H. Lu, ''Non-perturbative chiral corrections for lattice QCD,'' hep-ph/9905414.
[7] D. B. Leinweber, A. W. Thomas, K. Tsushima, and S. V. Wright, Phys. Rev. D **61**, 074502 (2000).
[8] D. B. Leinweber, A. W. Thomas, K. Tsushima, and S. V. Wright, Nucl. Phys. B (Proc. Suppl.) **83–84**, 179 (2000).
[9] A. W. Thomas, D. B. Leinweber, K. Tsushima, and S. V. Wright, Nucl. Phys. **A663–664**, 973 (2000).
[10] T. D. Cohen and D. B. Leinweber, Comments Nucl. Part. Phys. **21**, 137 (1993); A. W. Thomas, Aust. J. Phys. **44**, 173 (1991).
[11] S. R. Sharpe, Phys. Rev. D **56**, 7052 (1997); J. N. Labrenz and S. R. Sharpe, *ibid.* **54**, 4595 (1996); Nucl. Phys. B (Proc. Suppl.) **34**, 335 (1994).
[12] Particle Data Group, C. Caso *et al.*, Eur. Phys. J. C **3**, 1 (1998).
[13] D. B. Leinweber, R. M. Woloshyn, and T. Draper, Phys. Rev. D **43**, 1659 (1991).
[14] D. B. Leinweber, Phys. Rev. D **45**, 252 (1992).
[15] D. B. Leinweber, T. Draper, and R. M. Woloshyn, Phys. Rev. D **46**, 3067 (1992).
[16] D. B. Leinweber, Phys. Rev. D **47**, 5096 (1993).
[17] D. B. Leinweber, Nucl. Phys. B (Proc. Suppl.) **34**, 383 (1994).
[18] D. B. Leinweber, Nucl. Phys. **A585**, 341C (1995).
[19] M. F. Golterman and K. Leung, Phys. Rev. D **57**, 5703 (1998); M. F. Golterman, Acta Phys. Pol. B **25**, 1731 (1994).
[20] N. Cabibbo and E. Marinari, Phys. Lett. **119B**, 387 (1982).
[21] B. Efron, SIAM Rev. **21**, 460 (1979).
[22] S. Gottlieb, P. B. MacKenzie, H. B. Thacker, and D. Weingarten, Nucl. Phys. **B263**, 704 (1986).
[23] S. J. Dong, K. F. Liu, and A. G. Williams, Phys. Rev. D **58**, 074504 (1998).